

neural network application, forecasting, sutures tensile

Robert KARPIŃSKI*, Jakub GAJEWSKI*
Jakub SZABELSKI**, Dalibor BARTA***

APPLICATION OF NEURAL NETWORKS IN PREDICTION OF TENSILE STRENGTH OF ABSORBABLE SUTURES

Abstract

The paper presents results of research on neural network application in forecasting the tensile strength of two types of sutures. The preliminary research was conducted in order to establish the accuracy of the proposed method and will be used for formulating further research areas. The neural network enabled evaluation of suture material degradation after 3-to-6-days' exposure to Ringer's solution. The encountered problems regarding inaccuracies show that developing a single model for sutures may be difficult or impossible. Therefore future research should be conducted for a single type of sutures only and require applying additional parameters for the neural network.

1. INTRODUCTION

Surgical sutures are widely used in numerous fields of specialist medicine, and are mainly applied to join the edges of wounds resulting from a surgical intervention or an accident. Non-absorbable sutures retain their mechanical properties over the entire period of implantation until removed from the tissue,

* Lublin University of Technology, Faculty of Mechanical Engineering, Department of Machine Design and Mechatronics, Nadbystrzycka 36, 20-618 Lublin, Poland, r.karpinski@pollub.pl, j.gajewski@pollub.pl

** Lublin University of Technology, Faculty of Mechanical Engineering, Institute of Technological Systems of Information, Nadbystrzycka 36, 20-618 Lublin, Poland, j.szabelski@pollub.pl

*** University of Zilina, Faculty of Mechanical Engineering, Univerzitna 1, 01026 Zilina, Slovak Republic, dalibor.barta@fstroj.uniza.sk

whereas absorbable sutures lose their initial properties to the point of complete absorption. In the processes of biodegradation and absorption two major parameters are considered: absorption of suture mass and retention of initial tensile strength (Zapalski & Chęciński, 1999; Karpiński, Szabelski & Maksymiuk, 2017; Karpiński, Górnjak, Szabelski & Szala, 2016a). Synthetic absorbable sutures become absorbed in the process of hydrolytic decomposition of the suture material. Premature strength loss, on account of suture material absorption occurring before the healing process completes, results in wound dehiscence. On the other hand, excessively low tensile properties may contribute to the suture acting like a surgical knife, cutting through surrounding tissues. It is therefore critical to the applicability of sutures that their selection is suitable to purpose requirements (Zapalski & Chęciński, 1999; Karpiński, Górnjak, Szabelski & Szala, 2016b). As in other material testing applications, computational methods may aid testing the changes in strength profile of selected suture materials. The aim of this preliminary study is to assess the suitability of *Radial Basis Function* Networks (RBF) in prediction of suture strength (Luo, 2017; Youshia, Ali & Lamprecht, 2017; Lv & Zheng, 2017; Hasnaoui, Krea & Roizard, 2017).

1.1. Radial Basis Function Networks

Radial basis functions neural networks (RBF) consist of a single hidden layer with radial neurons and the linear output layer (including scalar product). The hidden layer consists of radial neurons which – in the predicting strength case – model the Gaussian response surface. A function of any shape can be modelled using only one hidden layer. This results from the fact that the function is of a nonlinear character. In order for the network to create an effective model of a given function, it is necessary to ensure that the network's system has a sufficient number of radial neurons. With a suitable number of radial neurons, each important detail of the function being modelled can be assigned a relevant radial neuron, which leads to producing a solution that reflects the applied function with a satisfactory accuracy. The publications supporting the scientific achievement present the conclusions about the selection of signal features as input variables in RBF systems, comparing them to the previously used network models (Gajewski, Golewski & Sadowski, 2017).

In radial basis functions, for the input vector q , the hidden neuron realises the radial change around a given centre k function $\varphi(q) = \varphi(\|q-k\|)$, where non-zero values occur only in the vicinity of the centre. Based on the hidden neurons radially reflecting the space around individual points, the input neuron reflects a multidimensional space. The approximate output of an RBF, for the K basis functions can be written as:

$$y = \sum_{i=1}^N w_i \varphi(\|g - k_i\|) \quad (1)$$

where c_i is a set of determinable centres ($i = 1, 2, 3, \dots, N$).

For the applied Gaussian radial basis function at point c_i , we can define:

$$\varphi(g) = \varphi(\|g - k_i\|) = \exp\left(-\frac{\|g - k_i\|^2}{2\sigma_i^2}\right) \quad (2)$$

where σ_i is a parameter which determines width of the function.

2. ABSORBABLE SURGICAL SUTURES

What is considered an absorbable suture material is the one that is subject to loss of mechanical properties, predominantly tensile strength, over a certain period of time in the body. Degradation of suture material as a result of various enzymatic reactions commences upon application of the stitch (Zapalski & Chęciński, 1999; Zurek, Kajzer, Basiaga & Jendruś, 2016). In the literature the term “*enzymatic degradation*” tends to be used to refer to decomposition of absorbable protein sutures, such as catgut, whereas synthetic suture material degradation occurs as a result of hydrolysis. As mentioned, the process of degradation begins immediately after inserting the suture material into the tissue and is complete after the period of 15–20 weeks. It ought to be remarked that hydrolysis is also catalysed by esterase enzyme (& Chęciński, 1999; Bollom & Meister, 2013; Casey & Lewis, 1986). Absorbable surgical sutures are also divided according to their mass absorption profile into: short-term, medium-term and long-term absorption sutures (Table 1).

Tab. 1. Classification of sutures according to mass absorption profile

| Mass absorption | 50% of initial tensile strength | Complete mass absorption |
|--------------------|---------------------------------|--------------------------|
| Short-term | 5–7 days | 42–56 days |
| Medium-term | 14–21 days | 60–90 days |
| Long-term | 28–35 days | 180–210 days |
| Extremelylong-term | 90 days | approx. 390 days |

It is highly important to differentiate between the complete suture mass absorption time and the tensile strength retention time, as it is the latter that provides critical information regarding absorbable suture applicability (Zapalski & Chęciński, 1999).

3. RELATIVE TENSILE STRENGTH OF SURGICAL SUTURES

To determine the impact of selected environmental factors on mechanical properties of surgical sutures physical tests were carried out. The study consisted in loading the suture material in tension to measure its linear tensile strength immediately after unpacking (pre-immersion), and collating the results with the second group of suture samples that were exposed to Ringer's solution for a particular period of time (post-immersion). The sutures were tested and stored at a temperature of 22°C.

There were two different types of short-term absorbable surgical sutures selected for testing. They were divided according to absorption time in the body into non-absorbable and absorbable sutures. The intervals between subsequent tensile strength tests reflected periods of mass suture absorption declared by particular manufacturers. The tests employed Ringer's solution, *i.e.* an isotonic solution, of identical osmotic potential as plasma, 1000 ml of which contains 8.6 g of sodium chloride, 0.3 g of potassium chloride, 0.33 g of calcium chloride dihydrate which corresponds to the following electrolyte levels: sodium – 147 mmol/l, potassium – 4 mmol/l, calcium – 2.2 mmol/l, chlorides – 156 mmol/l. The sutures were cut into 20 cm long samples. The diameter was measured with a micrometer by MIB, model *IP 54* with the accuracy of 0.001 mm. Afterwards, the measured tensile strength was compared with the one provided on the packaging.

The testing was carried out on a test set-up comprising MTS Bionix – Servohydraulic Test System universal testing machine located in the Institute of Technological Systems of Information (fig. 1). MTS TestWorks software allowed us to adjust the tensile loading speed according to the structure of the suture under examination – 10 mm/min for multifilament and 25 mm/min for monofilament materials. The test was automatically stopped when the load dropped by 75% at a short interval (suture failure).



Fig. 1. a) MTS Bionix material testing machine, b) the tensile strength test gripping system

The statistical analysis to determine discrepancies in the results obtained from the strength tests and the neural network prediction was carried out by means of Statistica 12.5 software, at a standard significance level $\alpha = 0.05$ (Krysicki, Bartos, Dyczka, Królikowska & Wasilewski, 1999; Rabiej, 2012).

In order to verify whether the scatter of particular strength test results corresponds to the normal distribution, we employed three tests: Kolmogorov-Smirnov tests, Lilliefors test and Shapiro-Wilk W test.

The analysis of equality of variances was carried out with three tests: F (Fisher's exact test), Levene's test and Brown-Forsythe test. For the results exhibiting normal distribution and equal variances – for the analysis of equality of means of relative tensile strength of surgical sutures at the specified significance level Student's T test was employed. In the case of results characterised by normal distribution but showing no equality of variances, the equality of mean relative tensile strength values was conducted by means of Student's T-test with separate variances adjustment (Cochran-Cox test) (Krysicki et al., 1999, Rabiej, 2012).

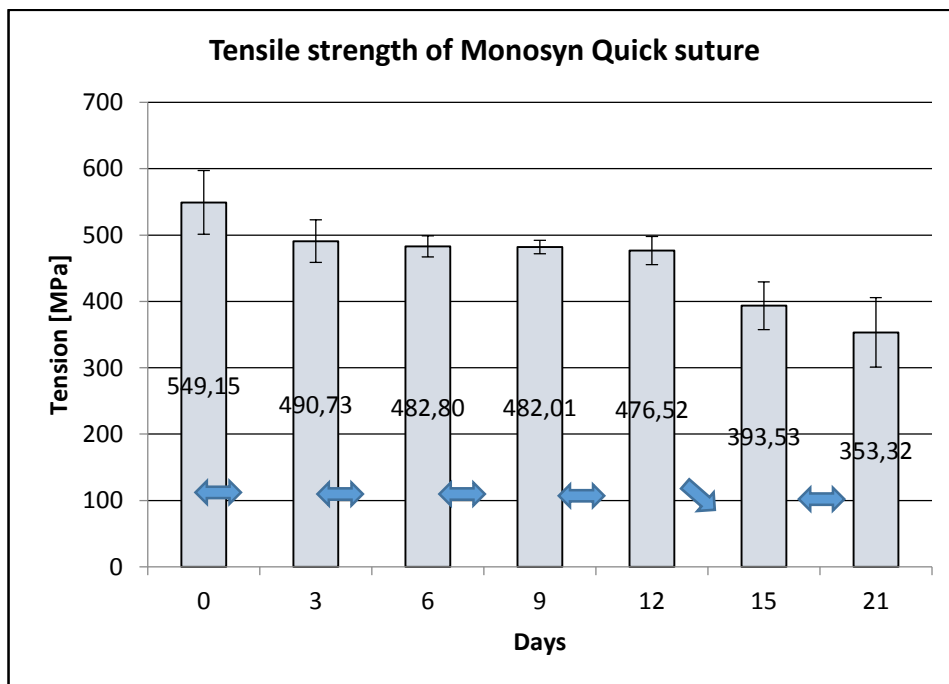


Fig. 2. Experimental results of tensile strength of Monosyn Quick sutures

The statistical analysis conducted for the Monosyn Quick sutures (fig. 2) showed no substantial differences between the pre-immersion (D0) and post-immersion sample series, including samples exposed to solution for three (D3),

six (D6), nine (D9) and 12 days (D12). Major discrepancies, however, occurred between the series tested during the 12th (D12) and 15th (D15) day of immersion. There were no significant differences between the series under examination during the 15th (D15) and 21st (D21) day in the solution either.

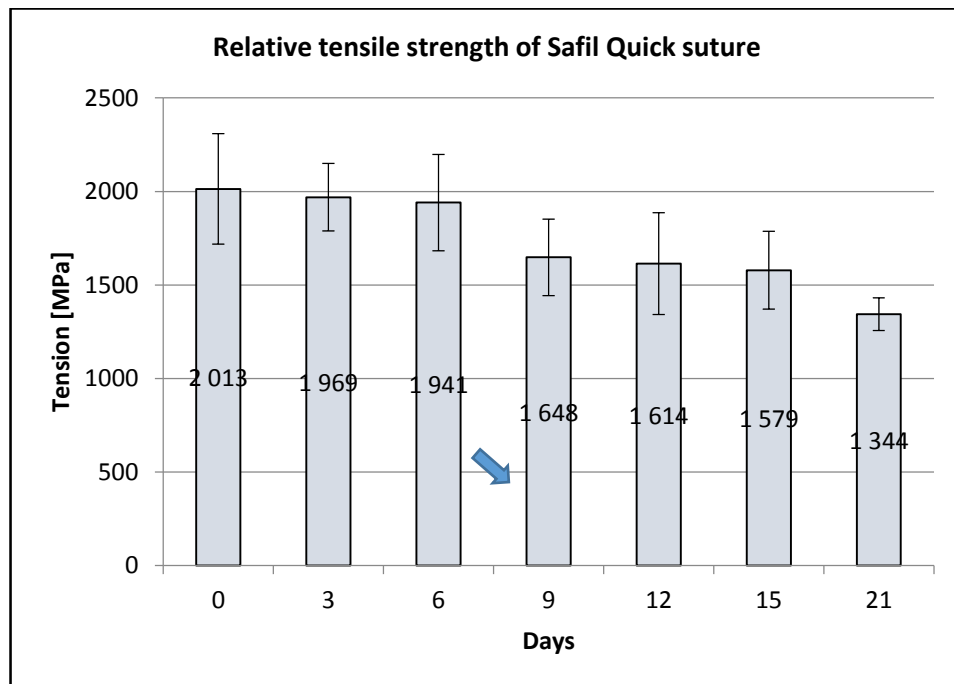


Fig. 3. Experimental results of tensile strength of Safil Quick sutures

The statistical analysis of Safil Quick sutures (fig. 3) showed no substantial differences between the pre-immersion samples (D0), including samples exposed to the solution for three days (D3) and six days (D6). Major discrepancies, however, occurred between the series tested during the 6th (D6) and 9th (D9) day of immersion. There were no significant differences between the series under examination during the 9th (D9), 12th (D12), 15th (D15) and 21st (D21) day in the solution.

4. RESULTS FROM NUMERICAL TESTS

The numerical part of this study consisted in applying artificial neural networks in prognosis of braking load of suture samples at later stages of material degradation, which were not subjected to experimental testing (Fig. 4). The numerical study was conducted by means of Statistica 13 software, which offers artificial neural network designing solutions.

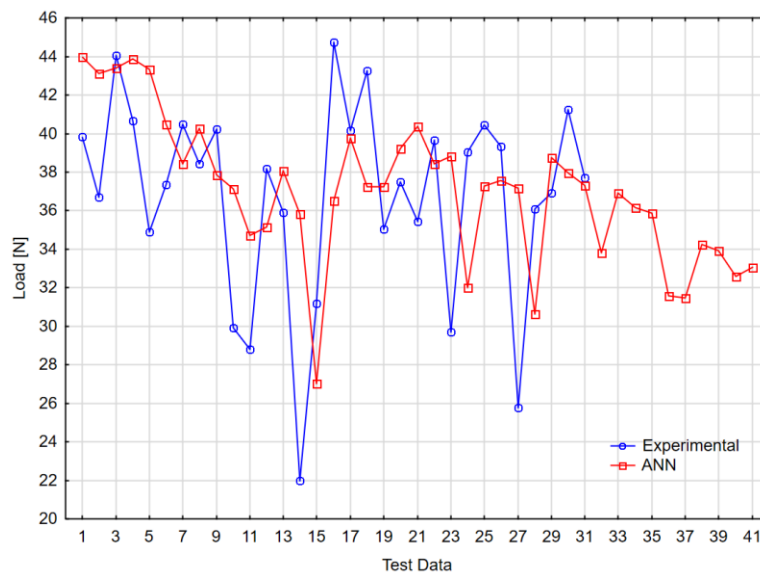


Fig. 4. Results of prognosis for Monosyn Quick suture

The figure above shows the lookahead of Monosyn Quick suture strength, evaluated by neural network. Six inputs resulted from the number of lag samples, which provided the base for further prognosis. The hidden layer consisted of 5 neurons. The data presented in the diagram show slight decrease in suture strength at subsequent stages of suture material deterioration. Although burdened with uncertainty, look ahead in neural networks indicates deterioration of tensile strength of samples in subsequent steps of the numerical experiment. The presented method may prove particularly useful in samples showing slight changes in parameters.

Tab. 2. Summary of Safil Quick network

| Summary of active networks (Safil Quick / Days) | | | | | |
|---|-----------------------|----------------------------|----------------------------|-----------------------------|--|
| Quality (training) | | Quality (testing) | | Quality (validation) | |
| 0.624576 | | 0.682461 | | 0.785921 | |
| Error (training) | | Error (testing) | | Error (validation) | |
| 13.19405 | | 10.42415 | | 3.045410 | |
| Training algorithm | Error function | Activation (hidden) | Activation (output) | | |
| RBFT | SOS | Gaussian | Linear | | |

Table 2 shows network training quality for the training, validation and testing sets, as well as training algorithms, error function and neuron activation. The division into testing and validation sub-sets was conducted at random. The presence of both these sets is necessary to conduct further network training with immediate validation of outputs. The reliability of the network is determined by the final set of data. High discrepancy in the results of training is likely to be the consequence of the small amount of experimental data, which is shown also in Fig. 5. The graphs of breaking loads, obtained from the experimental data and from the RBF network prognosis, show certain discrepancies of the data sets. Further studies with a larger sample set and higher sampling frequency are required to determine the efficacy of the method. The graph shows certain data generalisation, which must be applied given the character of the experiment, however, the correct prognosis trend is retained.

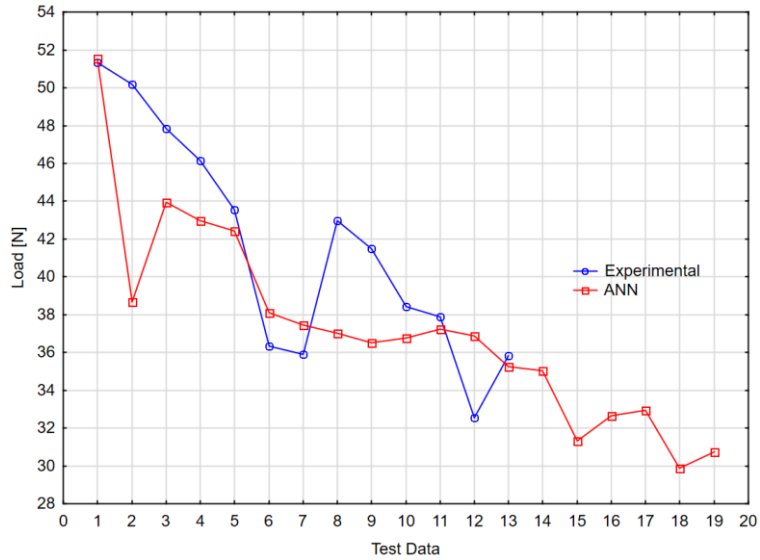


Fig. 5. Results of prognosis for Safil Quick suture

Tab. 3. Network weights for network, modelling the Safil Quick suture

| Weight ID | Network weights | |
|-----------|----------------------------------|---------------|
| | Connections | Weighted sums |
| 1 | monosyn-1 --> hidden neuron 1 | -0.041493 |
| 2 | monosyn-1 --> hidden neuron 2 | -0.061277 |
| 3 | monosyn-1 --> hidden neuron 3 | -0.062243 |
| 4 | monosyn-1 --> hidden neuron 4 | 0.635251 |
| 5 | monosyn-2 --> hidden neuron 1 | 0.665310 |
| 6 | monosyn-2 --> hidden neuron 2 | 0.596699 |
| 7 | monosyn-2 --> hidden neuron 3 | -0.276709 |
| 8 | monosyn-2 --> hidden neuron 4 | 0.109763 |
| 9 | monosyn-3 --> hidden neuron 1 | -0.047365 |
| 10 | monosyn-3 --> hidden neuron 2 | 0.648808 |
| 11 | monosyn-3 --> hidden neuron 3 | 0.735964 |
| 12 | monosyn-3 --> hidden neuron 4 | 0.635251 |
| 13 | radial deviation hidden neuron 1 | 0.291209 |
| 14 | radial deviation hidden neuron 2 | 0.081621 |
| 15 | radial deviation hidden neuron 3 | 0.291209 |
| 16 | radial deviation hidden neuron 4 | 0.081621 |
| 17 | hidden neuron 1 --> monosyn | -0.021130 |
| 18 | hidden neuron 2 --> monosyn | 0.001865 |
| 19 | hidden neuron 3 --> monosyn | -0.151329 |
| 20 | hidden neuron 4 --> monosyn | 0.005065 |
| 21 | hidden shift --> monosyn | 0.204858 |

RBF network results for Monosyn Quick suture are show in Table 4.

Tab. 4. Summary of Monosyn network

| Summary of active networks (Monosyn2017 sutures) | | | | | |
|---|-----------------------|----------------------------|----------------------------|-----------------------------|--|
| Quality (training) | | Quality (testing) | | Quality (validation) | |
| 0.841304 | | 0.765371 | | 0.829250 | |
| Error (training) | | Error (testing) | | Error (validation) | |
| 5.074944 | | 7.207897 | | 13.54326 | |
| Training algorithm | Error function | Activation (hidden) | Activation (output) | | |
| RBFT | SOS | Gaussian | Linear | | |

The generated network error was 80%.

5. SUMMARY

This paper presents the results from the preliminary study evaluating the application of neural networks in prediction of surgical suture strength. The main objective of the study was to verify the applicability of the method for the given purpose and to pave the way for future studies. In both tested sutures, Monosyn Quick and Safil Quick, the Radial Basis Function Network exhibited good results in prediction of immediate relative tensile strength of the suture material, i.e. within the period of 3-6 days' immersion in Ringer's solution. The diagrams show that despite slight discrepancies the neural network is capable of predicting suture material degradation at a good level of certainty. The two suture materials analysed in the study exhibit slight differences in their absorption profile, which proves quite problematic in terms of developing a universal model of neural network for the strength prediction of all suture material types. It becomes evident that different suture material will require a separate neural network. In order for the future stages of this study to compensate for the limited application of neural networks, an extensive database of surgical suture materials should be created to provide a wide array of both suture material types and number. In terms of directions for future research, further work should establish the criteria for designing surgical sutures for particular purpose requirements. This will necessitate determining factors that affect mechanical properties of sutures to the greatest extent.

REFERENCES

- Bollom, T., & Meister, K. (2013). Surgical principles: biodegradable materials in sports Medicine. In J. C. DeLee, D. J. Drez, & M. D. Miller (Eds.), *DeLee & Drez's Orthopaedic Sports Medicine: Principles and Practice. 2nd edition*. Philadelphia, PA: Saunders.
- Casey, D. J., & Lewis, O.G. (1986). Absorbable and nonabsorbable sutures. In A.F. von Recum (Ed.), *Handbook of biomaterials. Scientific and clinical testing of implant materials*. New York: Macmillan.
- Gajewski, J., Golewski, P., & Sadowski, T. (2017). Geometry optimization of a thin-walled element for an air structure using hybrid system integrating artificial neural network and finite element method. *Composite Structures*, 159, pp. 589–599. doi:10.1016/j.compstruct.2016.10.007
- Hasnaoui, H., Krea, M., & Roizard, D. (2017). Neural networks for the prediction of polymer permeability to gases. *Journal of Membrane Science*, 541, 541–549. doi:10.1016/j.memsci.2017.07.031
- Karpiński, R., Górniak, B., Szabelski, J., & Szala, M. (2016b). Charakterystyka i podział materiałów szwanych, In B. Zdunek, & M. Szklarczyk (Eds.), *Wybrane zagadnienia z biologii molekularnej oraz inżynierii materiałowej* (pp. 127–139). Lublin: Wydawnictwo Naukowe TYGIEL Sp. z o. o.
- Karpiński, R., Górniak, B., Szabelski, J., & Szala, M. (2016a). Historia chirurgii i materiałów szwanych, In B. Zdunek, & M. Szklarczyk (Eds.), *Wybrane zagadnienia z biologii molekularnej oraz inżynierii materiałowej* (pp. 140–150). Lublin: Wydawnictwo Naukowe TYGIEL Sp. z o. o.
- Karpiński, R., Szabelski, J., & Maksymiuk, J. (2017). Effect of Ringer's Solution on Tensile Strength of Non-Absorbable, Medium- and Long-Term Absorbable Sutures. *Advances in Science and Technology Research Journal*, 11(4), 11-20. doi:10.12913/22998624/76084
- Krysicki, W., Bartos, J., Dyczka, W., Królikowska, K., & Wasilewski, M. (1999). *Rachunek prawdopodobieństwa i statystyka matematyczna w zadaniach. część II. Statystyka matematyczna. Wydanie Szóste*. Warszawa: Wydawnictwo Naukowe PWN.
- Lv, H., & Zheng, Y. (2017). A newly developed tridimensional neural network for prediction of the phase equilibria of six aqueous two-phase systems. *Journal of Industrial and Engineering Chemistry*, 57, 377–386. doi:10.1016/j.jiec.2017.08.046
- Rabiej, M. (2012). *Statystyka z programem Statistica*. Gliwice: Helion.
- Youshia, J., Ali, M. E., & Lamprecht, A. (2017). Artificial neural network based particle size prediction of polymeric nanoparticles. *European Journal of Pharmaceutics and Biopharmaceutics*, 119, 333–342. doi: 10.1016/j.ejpb.2017.06.030
- Luo, Y. (2017). Recurrent neural networks for classifying relations in clinical notes. *Journal of Biomedical Informatics*, 72, 85–95.
- Zapalski, S., & Chęciński, P. (1999). *Szwy chirurgiczne: wybrane problemy*. Bielsko-Biała: Alfa-Medica Press.
- Zurek, M., Kajzer, A., Basiaga, M., & Jendruś, R. (2016). Właściwości wytrzymałościowe wybranych polimerowych nici chirurgicznych. *Polimery*, 61 (5), 334–338. doi:10.14314/polimery.2016.334